Behavioral/Systems/Cognitive

IκB Kinase Regulates Social Defeat Stress-Induced Synaptic and Behavioral Plasticity

Daniel J. Christoffel,[1] Sam A. Golden,[1] Dani Dumitriu,[1] Alfred J. Robison,[1] William G. Janssen,[1] H. Francisca Ahn,[1] Vaishnav Krishnan,[3] Cindy M. Reyes,[1] Ming-Hu Han,[1,2] Jessica L. Ables,[3] Amelia J. Eisch,[3] David M. Dietz,[1] Deveroux Ferguson,[1] Rachael L. Neve,[4] Paul Greengard,[5] Yong Kim,[5] John H. Morrison,[1] and Scott J. Russo[1]

[1]Fishberg Department of Neuroscience and Friedman Brain Institute and [2]Department of Pharmacology and Systems Therapeutics, Mount Sinai School of Medicine, New York, New York 10029, [3]Department of Psychiatry, University of Texas Southwestern Medical Center, Dallas, Texas 75390, [4]Massachusetts Institute of Technology, Cambridge, Massachusetts 02139, and [5]Laboratory of Molecular and Cellular Neuroscience, The Rockefeller University, New York, New York 10065

The neurobiological underpinnings of mood and anxiety disorders have been linked to the nucleus accumbens (NAc), a region important in processing the rewarding and emotional salience of stimuli. Using chronic social defeat stress, an animal model of mood and anxiety disorders, we investigated whether alterations in synaptic plasticity are responsible for the long-lasting behavioral symptoms induced by this form of stress. We hypothesized that chronic social defeat stress alters synaptic strength or connectivity of medium spiny neurons (MSNs) in the NAc to induce social avoidance. To test this, we analyzed the synaptic profile of MSNs via confocal imaging of Lucifer-yellow-filled cells, ultrastructural analysis of the postsynaptic density, and electrophysiological recordings of miniature EPSCs (mEPSCs) in mice after social defeat. We found that NAc MSNs have more stubby spine structures with smaller postsynaptic densities and an increase in the frequency of mEPSCs after social defeat. In parallel to these structural changes, we observed significant increases in IκB kinase (IKK) in the NAc after social defeat, a molecular pathway that has been shown to regulate neuronal morphology. Indeed, we find using viral-mediated gene transfer of dominant-negative and constitutively active IKK mutants that activation of IKK signaling pathways during social defeat is both necessary and sufficient to induce synaptic alterations and behavioral effects of the stress. These studies establish a causal role for IKK in regulating stress-induced adaptive plasticity and may present a novel target for drug development in the treatment of mood and anxiety disorders in humans.

Introduction

Mood and anxiety disorders are prevalent psychiatric conditions affecting one in six people during their lifetime, and the experience of chronic stress has been shown to be a major precipitating factor in both (Kessler et al., 2005). Dendritic spine plasticity is a critical element of experience-dependent reorganization of the brain (Shepherd et al., 2003; Bourne and Harris, 2007; Holtmaat and Svoboda, 2009), and maladaptive changes in spines are suggested to underlie neuropsychiatric disorders, such as depression, anxiety, and drug addiction (Berton and Nestler, 2006; Kauer and Malenka, 2007; Russo et al., 2010). Dysfunction of the mesolimbic dopaminergic reward pathway, including the ventral tegmental area (VTA) dopaminergic cells projecting to the nucleus accumbens, is linked to these neuropsychiatric disorders, which are characterized by altered motivational states. Interestingly, addictive drugs and stress can similarly cause acute alterations to the synaptic properties of VTA dopamine neurons (Saal et al., 2003), suggesting that common neuroadaptations may partly explain the pathology underlying both disorders.

Chronic social defeat stress models the behavioral features of depression and anxiety, such as social avoidance, anhedonia, and hyperarousal (Berton et al., 2006; Krishnan et al., 2007). Interestingly, similar to humans, social defeat only induces aspects of depression-like behavior in a subset of susceptible animals, suggesting that there are individual differences in coping responses (Krishnan et al., 2007). In this study, the authors reported increased firing rates of VTA dopaminergic neurons after social defeat only in susceptible mice, an effect that is accompanied by increased release of brain-derived neurotrophic factor (BDNF) to projection regions, including the nucleus accumbens (NAc). However, what effect social defeat and this altered input from the VTA have on NAc medium spiny neurons (MSNs) in susceptible mice is still unclear. A variety of stress procedures have been shown to result in significant alterations to the neuronal morphology of a variety of cell types (Radley et al., 2006; Goldwater et al., 2009; Shansky and Morrison, 2009). BDNF and its downstream targets, such as IκB kinase (IKK)–nuclear factor κB (NFκB), have been shown to be an important regulator of neuronal structure (Chakravarthy et al., 2006; Russo et al., 2009a)

Received Sept. 10, 2010; revised Oct. 8, 2010; accepted Oct. 20, 2010.

This work was supported by a grant from the National Alliance for Research on Schizophrenia and Depression (S.J.R.). D.J.C., D.D., A.J.R., V.K., J.H.M., and S.J.R. designed the experiments. D.J.C., S.A.G., D.D., A.J.R., W.G.J., H.F.A., V.K., C.M.R., M.-H.H., J.L.A., A.J.E., D.M.D., D.F., R.L.N., P.G., Y.K., and S.J.R. performed and analyzed the experiments. D.J.C. and S.J.R. wrote the manuscript.

The authors declare no competing financial interests.

Correspondence should be addressed to Scott J. Russo, Fishberg Department of Neuroscience, Mount Sinai School of Medicine, One Gustave L. Levy Place, Box 1065, New York, NY 10029-6574. E-mail: scott.russo@mssm.edu.

DOI:10.1523/JNEUROSCI.4763-10.2011

 0270-6474/11/310314-08$15.00/0

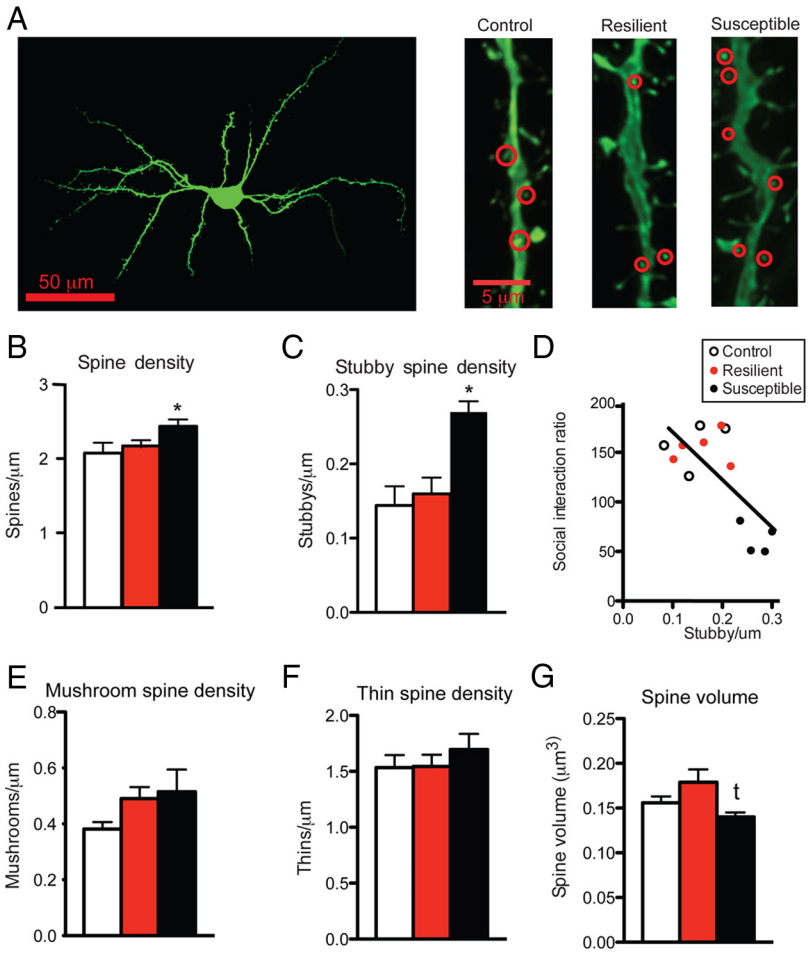

Figure 1. Chronic social defeat stress regulates spine morphology on NAc MSNs in susceptible mice. ***A***, Representative confocal *z*-stack images of a Lucifer-yellow-filled NAc MSN and selected dendritic segments. ***B***, ***C***, Stubby spines are circled in red. Chronic social defeat stress results in an increase total spine density (***B***) and stubby spine density (***C***). ***D***, Stubby spine density correlates with social interaction ratio. ***E***, ***F***, No changes were observed in mushroom (***E***) or thin (***F***) spines. ***G***, A trend toward a decrease in spine volume in susceptible mice was found. Data are represented as group means. Error bars represent SEM. $^{*}p < 0.05$, $^{t}p = 0.07$, one-way ANOVA, 56 neurons, $n = 4–5$ mice per group.

and may be a critical pathway affecting the synaptic profile of NAc MSNs after chronic social defeat stress.

A greater understanding of the molecular mechanisms mediating dendritic remodeling and its functional role in long-term social avoidance is critical to understanding, and possibly treating, maladaptive stress responses (Berton and Nestler, 2006). Therefore, we investigated changes in dendritic spine morphology, synapse size, and miniature EPSCs (mEPSCs) in NAc MSNs after social defeat. We further investigated the mechanisms of long-term social avoidance by targeting IKK, which is regulated by social defeat. We hypothesize that the induction of IKK is essential for social-defeat-induced synaptic plasticity and social avoidance.

Materials and Methods

Animals. Nine- to eleven-week-old C57BL/6J male mice (The Jackson Laboratory) ($n = 186$ mice) were used in all experiments. Four days before the beginning of experiments, all mice were singly housed and maintained on a 12 h light/dark cycle with *ad libitum* access to food and water. Behavioral assessments and tissue collection were performed 1 h into the animals' dark phase. Mouse procedures were performed in accordance with the Institutional Animal Care and Use Committee guidelines of the Mount Sinai School of Medicine.

Social defeat stress. Chronic social defeat stress was performed as described previously (Berton et al., 2006; Tsankova et al., 2006; Krishnan et al., 2007). Briefly, experimental C57BL/6J mice were exposed to a novel CD1 aggressor for 10 min daily over 10 consecutive days. CD1 mice 4–5 months old were selected for aggressive behavior based on criteria described previously (Berton et al., 2006). After 10 min of physical contact, experimental mice were removed and placed on the opposite side of the aggressor's home cage behind a "protective" partition that was perforated with holes to allow for sensory contact during the following 24 h. Control mice were housed two animals per cage under the same conditions as their experimental counterparts but without the presence of an aggressive CD1 mouse. Experimental mice were relocated to a new cage each day immediately before the social defeat. Twenty-four hours after the final social defeat, all mice were housed individually. To measure increased susceptibility to stress, we adapted a subthreshold "microdefeat" as described previously (Krishnan et al., 2007). Under these conditions, C57BL/6J mice were exposed to a novel CD1 aggressor for 5 min, followed by 5 min rest in the home cage. Exposure to the CD1 aggressor occurred three times with 5 min intervals between each exposure. Twenty-four hours later, mice were assessed using the social interaction test described below. Under control conditions, this subthreshold microdefeat protocol does not induce social avoidance.

Behavioral assessments. Social interaction was performed as described previously (Berton et al., 2006). Briefly, mice were placed into a novel arena with a small animal cage at one end. Their movement was monitored for 2.5 min in the absence of an aggressive CD1 mouse (used to determine baseline exploratory behavior), followed by 2.5 min in the presence of the caged aggressor. We measure the distance traveled (in centimeters) and duration spent in the interaction zone and corner zones (in seconds) using Ethovision 3.0 software (Noldus Information Technology). We calculated social interaction as a ratio of the time spent in the interaction zone with an aggressive mouse present over the time spent with the aggressive mouse absent and then multiplied by 100. All mice with a ratio above 100 were classified as resilient, and all mice with a ratio below 100 were classified as susceptible.

Stereotaxic surgery and viral gene transfer. Mice ($n = 71$ mice, 4–6 mice per group for structural studies and 12–13 mice per group for behavioral studies) were anesthetized with a mixture of ketamine (100 mg/kg) and xylazine (10 mg/kg) and positioned in a small-animal stereotaxic instrument (David Kopf Instruments), and the skull surface was exposed. Thirty-three-gauge syringe needles (Hamilton Co.) were used to bilaterally infuse 0.5 μl of virus (1.5×10^8 infectious units/ml) expressing a control green fluorescent protein (GFP) or either a dominant-negative (IKKdn) or constitutively active (caIKK) IKK mutant to activate or inhibit NFκB signaling, respectively, into the NAc (bregma coordinates: anteroposterior, +1.5 mm; mediolateral, +1.6 mm; dorsoventral, −4.4 mm) at a rate of 0.1 ml/min. All of these viral vectors have been tested and validated *in vivo* and *in vitro* (LaPlant et al., 2009; Russo et al., 2009b).

Perfusion and tissue processing. At 24 h after the social interaction test, mice were killed with a dose of 15% chloral hydrate and transcardially perfused with cold 1% paraformaldehyde in PBS, pH 7.4, followed by fixation with cold 4% paraformaldehyde with 0.125% glutaraldehyde in PBS. Brains were dissected and postfixed for 18 h in the same fixative. The iontophoretic cell loading procedure was performed as described previously (Radley et al., 2006; Goldwater et al., 2009). In brief, neurons in the

NAc shell were loaded with intracellular injections of 5% Lucifer yellow (Invitrogen) under a direct current of 1–6 nA for 10 min. Sections were then mounted on Superfrost Plus slides in Vectashield (Vector Laboratories) mounting medium and coverslipped before imaging.

Imaging and NeuronStudio. For spine analysis, dendritic segments 50–150 μm away from the soma were randomly chosen from either Lucifer-yellow-filled neurons (see Fig. 1*A*) or herpes simplex viral (HSV)-infected cells that express GFP (see Fig. 5*A*). Images were acquired on a confocal LSM 710 (Carl Zeiss) for morphological analysis as described previously (Radley et al., 2006). Neurons were selected from the medial dorsal aspect of the NAc shell. To qualify for spine analysis, dendritic segments had to satisfy the following requirements: (1) the segment had to be completely filled (all endings were excluded), (2) the segment must be at least 50 μm from the soma, and (3) the segment could not be overlapping with other dendritic branches (Radley et al., 2006). Dendritic segments were imaged using a 100× lens (numerical aperture 1.4; Carl Zeiss) and a zoom of 2.5. Pixel size was 0.03 μm in the *x–y* plane and 0.01 μm in the *z* plane. Images were taken with a resolution of 1024 × ~300 (the *y* dimension was adjusted to the particular dendritic segment to expedite imaging), pixel dwell time was 1.58 μm/s, and the line average was set to 4. An average of two dendrites per neuron on five neurons per animal (n = 13 mice, n = 4–5 mice per group) totaling ~3000 dendritic spines per experimental group were analyzed. For quantitative analysis of spine size, shape, and volume, NeuronStudio was used with the rayburst algorithm described previously (Rodriguez et al., 2008). NeuronStudio classifies spines as thin, mushroom, or stubby based on the following values: (1) aspect ratio, (2) head to neck ratio, and (3) head diameter. Spines with a neck can be classified as either thin or mushroom, and those without a significant neck are classified as stubby. Spines with a neck are labeled as thin or mushroom based on head diameter. These parameters have been verified by comparison with trained human operators.

Electron microscopy. Tissue was processed for electron microscopy (EM) ultrastructural analysis as described previously (Janssen et al., 2005). Briefly, mice (n = 13 mice, n = 4–5 mice per group) were anesthetized and perfused as described above. Brains were removed and post-fixed overnight in cold 4% paraformaldehyde with 0.125% glutaraldehyde in PBS. Coronal sections of the NAc, 1 mm thick, were isolated and cryoprotected in increasing solutions of glycerol (10–30%). Freeze substitution and low-temperature cryoembedding, using Lowicryl Resin (Electron Microscopy Sciences), were then performed. Ultrathin sections (90 nm) were cut with a diamond knife on an ultramicrotome (Reichert-Jung) and mounted on nickel slot grids using a Coat-Quick adhesive pen (Electron Microscopy Sciences). Ultrastructural analyses were performed on a Hitachi H-7000 electron microscope and imaged with a MEGAPlus model ES 4.0 digital camera. EM images were produced using Adobe Photoshop 7.0.

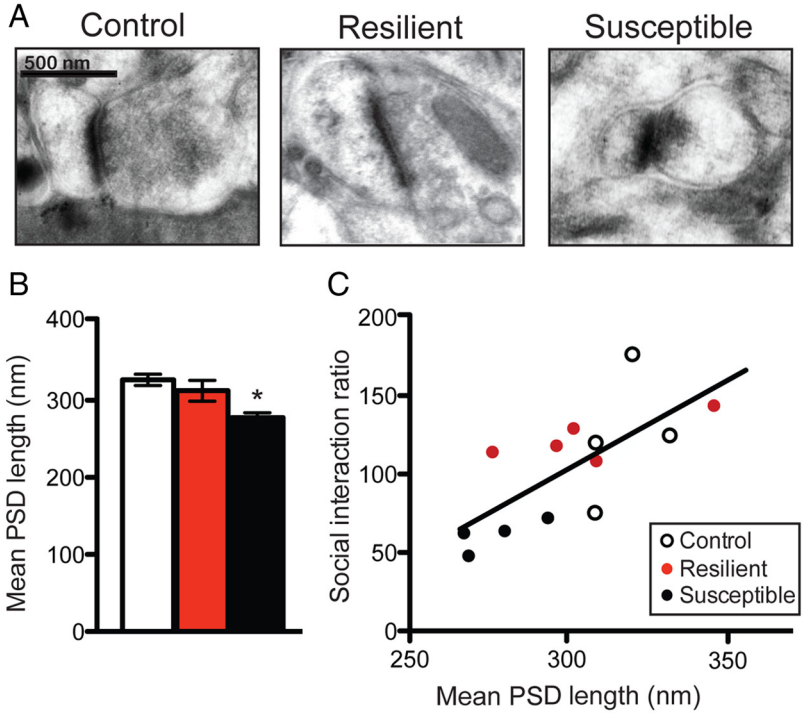

Figure 2. Chronic social defeat stress regulates the size of the PSD in susceptible mice. ***A***, Representative photomicrographs of excitatory synapses. ***B***, Susceptible animals have synapses with significantly smaller average PSD length. ***C***, As well, mean PSD length correlates with social interaction ratio. Data are represented as group means. Error bars represent SEM. *$p < 0.05$, one-way ANOVA, $n = 4–5$ mice per group.

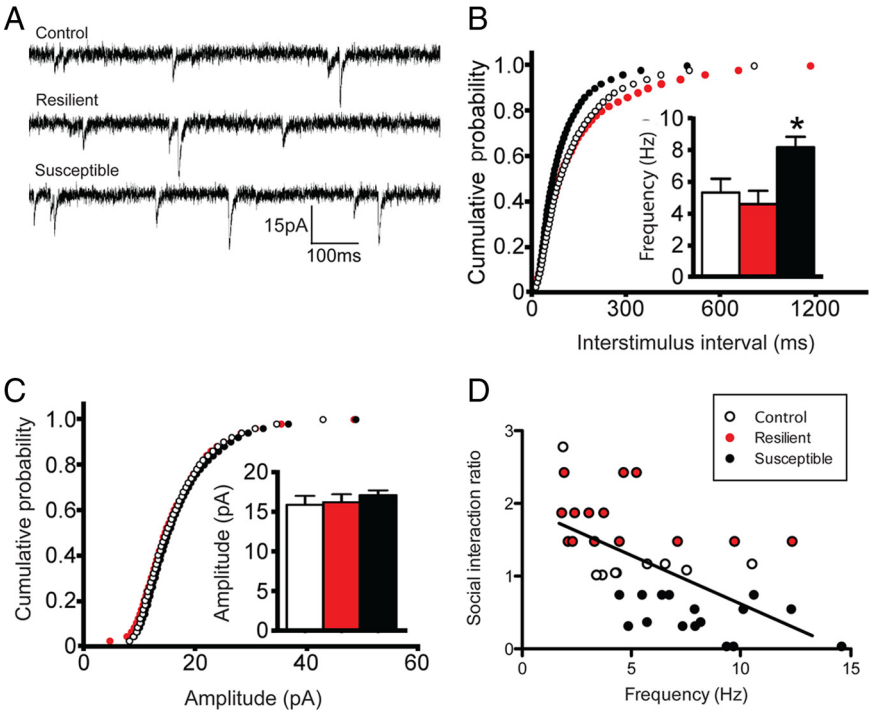

Figure 3. Chronic social defeat stress regulates synaptic transmission in susceptible mice. ***A***, Representative traces of mEPSCs. ***B***, Chronic social defeat stress increases mEPSC frequency only in susceptible animals. ***C***, No changes in amplitude were observed after chronic social defeat. Calibration: 15 pA, 100 ms. ***D***, mEPSC frequency also correlates with social interaction ratio. Data are represented as group means. Error bars represent SEM. *$p < 0.05$, one-way ANOVA, 39 neurons, $n = 4–6$ mice per group.

Ultrastructural analysis. Sampling fields from the NAc shell were chosen in a systematic random manner (Geinisman et al., 1996). Ultrathin sections were obtained from blocks of the medial dorsal NAc shell. Serial strips were taken, and three consecutive sections were used for estimates

of postsynaptic density (PSD) length. We measured the mean length of ~45 PSDs per animal in four to five animals per group. Asymmetric synapses were identified as having a PSD facing an axon terminal. Criteria for analysis were (1) synapses must be transversely and not tangentially cut, (2) synapses must show a clear PSD and synaptic cleft, and (3) synapses must appear in the second section of a series of three consecutive sections imaged. Measurements of maximal PSD length were obtained by taking the longest PSD identified in the strip of three serial sections (Nicholson and Geinisman, 2009). PSD length measurements were obtained in Adobe Photoshop.

Electrophysiology. All electrophysiological experiments were performed on control mice or those subjected to chronic (10 d) social defeat, 2–23 d after the last defeat episode ($n = 15$ mice, $n = 4–6$ mice per group,). Separate experimenters performed social defeat and electrophysiological recording, which were conducted blind to mouse phenotype. Coronal NAc slices (250 μm thick) were cut in ice-cold sucrose artificial CSF (ACSF) (in mM): 254 sucrose, 3 KCl, 1.25 NaH_2PO4, 10 D-glucose, 24 $NaHCO_3$, 2 $CaCl_2$, and 2 $MgSO_4$, pH 7.35 (oxygenated with 95% O_2 and 5% CO_2, 295–305 mOsm). After a 1 h recovery at 37°C in ACSF (254 mM sucrose replaced by 128 mM NaCl), electrophysiological recordings were performed at 30–32°C in ACSF containing 50 μM picrotoxin to block GABA-receptor-mediated IPSCs and 1.5 μM tetrodotoxin to block action potentials (Thomas et al., 2001). Patch pipettes (3–5 MΩ resistance) for whole-cell recordings were filled with an internal solution containing the following (in mM): 115 potassium gluconate, 20 KCl, 1.5 $MgCl_2$, 10 HEPES, 10 phosphocreatine, 2 ATP-Mg, 0.5 GTP, and 1 QX-314 [2(triethylamino)-*N*-(2,6-dimethylphenyl) acetamine] (a Na^+ channel blocker), pH 7.2 (280–290 mOsm). The shell of the NAc was identified under visual guidance using infrared differential interference contrast video microscopy with a 40× water-immersion objective (Olympus BX51-WI). Whole-cell voltage-clamp recordings were performed with a computer-controlled amplifier (MultiClamp 700B), digitized (Digidata 1440), and acquired with Axoscope 10.1 (Molecular Devices) at a sampling rate of 10 kHz. Only cells with resting membrane potential of −72 to −82 mV and that displayed inward rectification were included for analysis. Analysis was performed on 39 cells from 14 animals. The frequency and amplitude of mEPSCs were analyzed using Minianalysis software (Synaptosoft).

Western blotting. To ensure preservation of phospho-proteins in their *in vivo* phosphorylation state, the mice ($n = 26$ mice, $n = 8–10$ mice per group) were killed at 48 h after the last defeat by focused microwave irradiation (4.5–5 kW for 1.7 s) using a small-animal microwave (Murimachi Kikai). The brains were rapidly removed and chilled in ice-cold PBS for 5 min. The nucleus accumbens was dissected and stored at −80°C until assayed by immunoblotting. Frozen tissue samples were sonicated in lysis buffer [50 mM Tris-HCl, pH 7.5, 2 mM $MgCl_2$, 150 mM NaCl, 1% Triton X-100, protease inhibitor cocktail (Roche), 1 μM sodium vanadate, 30 mM sodium pyrophosphate, and 30 mM sodium fluoride]. The protein concentration in each sample was determined by the Bradford method (Bio-Rad). Equal amounts of protein sample were separated by SDS-PAGE (4–20% polyacrylamide gels) and transferred to nitrocellulose membranes. The membranes were immunoblotted using anti-IKKα (1:1000, Cell Signaling Technology), anti-IκBα (112B2, 1:1000; Cell Signaling Technology), and anti-phospho-Ser32/36–IκBα (5A5, 1:1000; Cell Signaling Technology). Antibody binding was detected using the enhanced chemiluminescence immunoblotting detection system after incubating membranes with horseradish peroxidase-linked goat anti-rabbit IgG (1:10,000) or anti-mouse IgG (1:5000) antibody (Pierce).

Statistical analysis. All data are expressed as the mean ± SEM. Mean differences between groups were determined using a Student's *t* test or a one- or two-way ANOVA, followed by Newman–Keuls *post hoc* tests when the main effect or interaction was significant at $p < 0.05$. Statistical analyses were performed using Prism 5.0 (GraphPad Software).

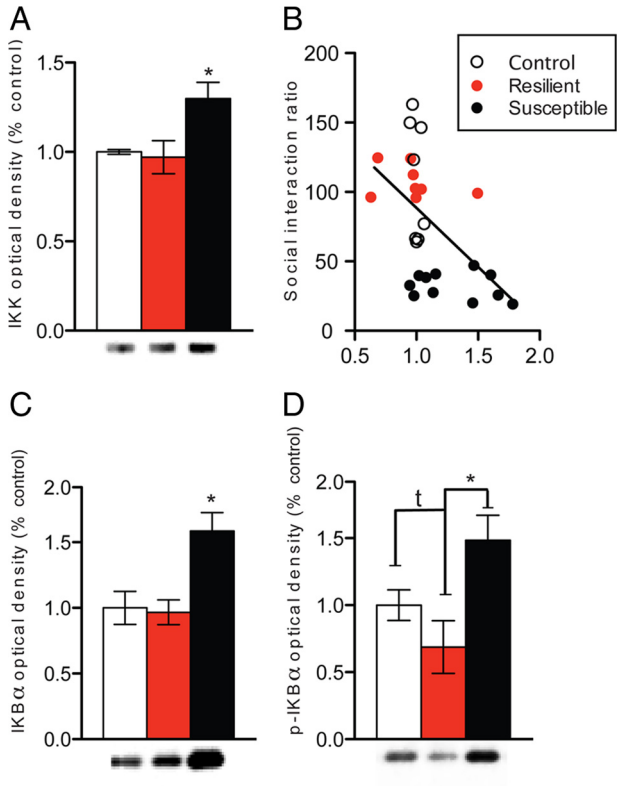

Figure 4. Chronic social defeat stress regulates levels of IKK. ***A***, Social defeat increases total levels of IKK protein. ***B***, Levels of IKK correlate with SI ratio. ***C***, ***D***, Levels of IκB (***C***) and phosphorylated IκB (p-IκB; ***D***), downstream targets of IKK, are significantly increased after chronic social defeat stress. All data are expressed as mean ± SEM optical density percentage control. $^*p < 0.05$, $^tp < 0.07$, one-way ANOVA, $n = 8–10$ mice per group.

Results

Social defeat stress increases stubby spine formation with smaller average PSDs

To study the effect of social defeat stress on spine morphology, we recreated three-dimensional dendritic segments of Lucifer-yellow-filled MSNs from susceptible and resilient mice and then performed semi-automated analysis of spine type with NeuronStudio (Rodriguez et al., 2008). We find a main effect of social defeat stress on total and stubby spine density on MSNs in the NAc shell and a trend toward a decrease in total spine head volume only in susceptible animals (one-way ANOVA: $F_{(2,12)} = 4.05$, $p < 0.05$; $F_{(2,12)} = 9.60$, $p = 0.005$; and $F_{(2,12)} = 3.45$, $p = 0.07$, respectively) (Fig. 1*B*,*C*,*G*). There were no changes observed in the density of thin or mushroom spines (Fig. 1*E*,*F*). Stubby spines are thought to be immature structures that have little or no spine neck and smaller PSDs (Harris and Kater, 1994; Shepherd et al., 2003; Schmidt and Eilers, 2009). We verified a main effect of stress on average PSD length, using serial section electron microscopy. Specifically, we found that susceptible mice have smaller PSDs than control and resilient mice (one-way ANOVA: $F_{(2,12)} = 5.28$, $p = 0.02$) (Fig. 2*B*). Interestingly, both stubby spine density and PSD length correlated with social interaction ratio ($r^2 = 0.65$, $p = 0.01$; $r^2 = 0.58$, $p = 0.002$, respectively) (Figs. 1*D*, 2*C*), suggesting that these synaptic changes are critical mediators of social avoidance. Given that, on average, the total dendritic length of an MSN is ~1000 μm, our observed change in spine density equates to an increase of ~130 spines per neuron, which could result in a large functional increase within the NAc (see Fig. 7). To confirm a functional change in the syn-

aptic properties of NAc MSNs, we measured mEPSCs after social defeat stress. We find a main effect of stress on the mEPSC frequency, but not amplitude, only in susceptible mice (one-way ANOVA: $F_{(2,38)} = 6.60$, $p = 0.0004$) (Fig. 3*B*,*C*), a measure that also correlates with social interaction ratio ($r^2 = 0.35$, $p < 0.0001$) (Fig. 3*D*). These data are consistent with NAc MSNs having more glutamatergic synapses, thus providing even greater functional relevance to these structural changes.

Social defeat stress induces an increase in IKK activity

Given the dramatic effects of social defeat stress on both structure and function of NAc MSNs, we next wanted to determine the mechanism and relevance of these structural changes in controlling social avoidance behavior. Previous studies have shown that IKK or its downstream target NFκB is critical in mediating cocaine-induced striatal plasticity and memory-related hippocampal plasticity (Meffert et al., 2003; Lubin and Sweatt, 2007; Russo et al., 2009b; Koo et al., 2010). Thus, we tested whether IKK also regulates social-defeat-induced dendritic spine plasticity and social avoidance behavior. We find a main effect of stress on total levels of IKK (one-way ANOVA: $F_{(2,26)} = 5.52$, $p = 0.02$) (Fig. 4*A*) and phosphorylated and total levels of IκB, downstream transcriptional and posttranslational targets of IKK, only in susceptible animals (one-way ANOVA: $F_{(2,26)} = 4.40$, $p = 0.03$; $F_{(2,26)} = 5.43$, $p = 0.01$, respectively) (Fig. 4*C*,*D*). Levels of IKK and social interaction ratio were also correlated ($r^2 = 0.2823$, $p = 0.004$) (Fig. 4*B*), providing additional evidence that IKK may induce synapse remodeling and lead to long-term social avoidance.

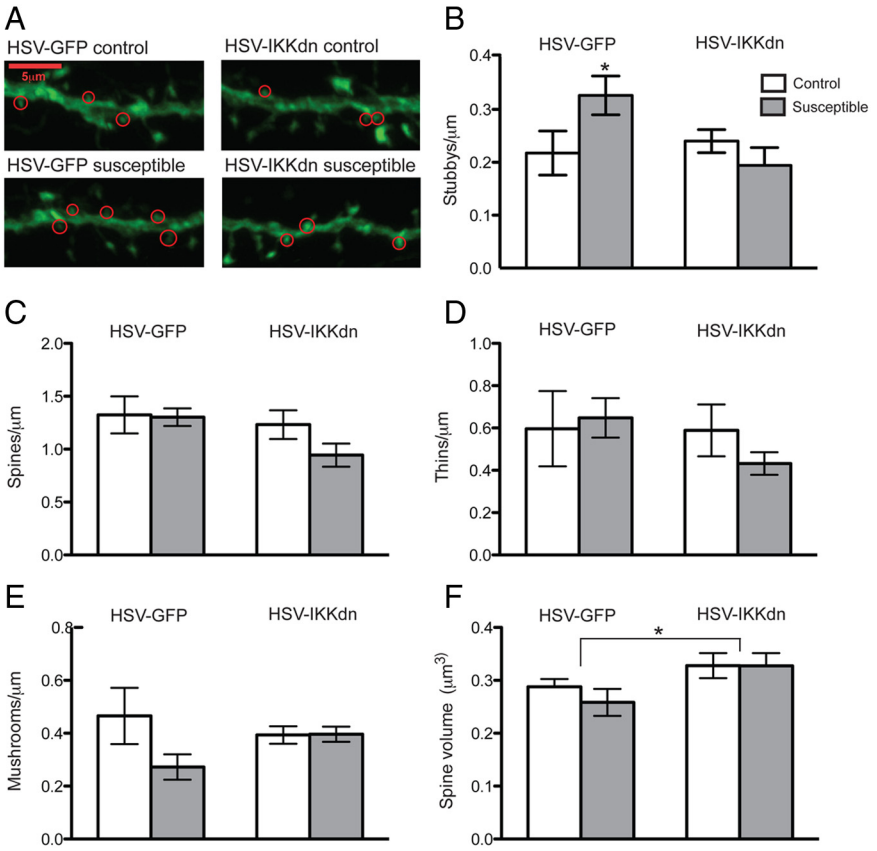

Figure 5. ***A***, Representative confocal *z*-stack images of viral-infected dendritic segments from MSNs. Stubby spines are circled in red. ***B–E***, Expression of IKKdn in MSNs is sufficient to reverse the induction of stubby spines after social defeat (***B***) but does not affect total (***C***), thin (***D***), or mushroom (***E***) density. ***F***, Expression of IKKdn causes an increase spine head volume regardless of group. Data are represented as group means. Error bars represent SEM. *$p < 0.05$, two-way ANOVA, 72 neurons, $n = 4–6$ mice per group.

IKK regulates social defeat stress-induced structural and behavioral plasticity

To prove that IKK is indeed regulating spine plasticity, we injected HSV vectors to express IKKdn after social defeat, only in susceptible mice. We find an interaction between virus and stress on stubby spines in which IKKdn reverses the formation of stubby spines in susceptible mice (two-way ANOVA: $F_{(1,15)} = 4.615$, $p < 0.05$) (Fig. 5*B*). Expression of IKKdn did not cause any significant differences in total, thin, or mushroom spine density (Fig. 5*C–E*). Although we did not notice an increase in total spine density, as we did in our Lucifer yellow studies, this may be attributable to a slight design modification to account for the transient nature of HSV expression. Here we injected HSVs after social defeat, requiring us to analyze 72 versus 48 h after the final stress. Given this caveat, we still observed an increase in stubby spines and a main effect of the virus, in which IKKdn increases spine head volume (two-way ANOVA: $F_{(1,15)} = 4.88$, $p < 0.05$) (Fig. 5*F*). This latter finding corroborates data from our EM and Lucifer yellow studies, which would imply that the opposite molecular change after chronic social defeat stress, increased IKK, would lead to decreased average spine volume or PSD size.

To provide functional evidence that IKK changes dendritic structure to mediate social-defeat-induced avoidance, we again injected IKKdn into NAc after chronic social defeat stress, only in susceptible mice, and found a significant interaction between stress and virus: IKKdn fully reverses social avoidance (two-way ANOVA: $F_{(1,44)} = 4.23$, $p < 0.05$) (Fig. 6*A*). We then expressed IKKca, which we have shown previously to increase the formation of new dendritic spines (Russo et al., 2009b) to artificially induce activity in naive mice and subjected them to a 1 d subthreshold microdefeat that does not normally induce social avoidance (Krishnan et al., 2007). We found an interaction between stress and virus on social interaction ratio, indicating a profound social avoidance in the IKKca group (two-way ANOVA: $F_{(1,48)} = 4.01$, $p < 0.05$) (Fig. 6*B*). These results show that IKK is both necessary and sufficient to produce a social avoidance phenotype.

Discussion

Social defeat induces the formation of new stubby spines with smaller PSDs and a functional increase in mEPSCs in NAc MSNs (Fig. 7). Interestingly, all of these measures of synaptic plasticity correlate with social avoidance, which suggests that these structural changes may be controlling this behavioral phenotype. As well, we found IKK to be upregulated in the NAc of susceptible

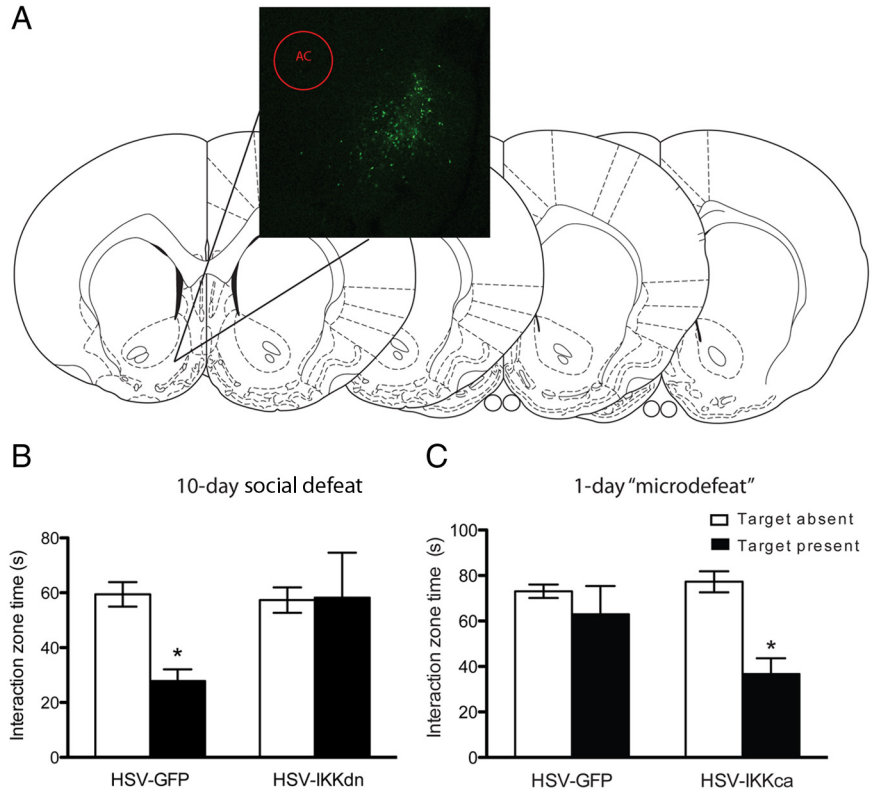

Figure 6. ***A***, Representative expression of HSV in NAc. GFP-labeled neurons in green show the area of infection, whereas representative slices from the mouse brain atlas of Paxinos and Franklin (1997) indicate the relative spread of HSV throughout the NAc. ***B***, Expression of IKKdn in NAc after 10 d social defeat reveres social avoidance ($n = 12$ mice per group. ***C***, Expression of IKKca before a 1 d subthreshold microdefeat induces a social avoidance phenotype ($n = 13$ mice per group). White and black bars represent interaction time when the target aggressor mouse is absent or present, respectively. Data are represented as group means. Error bars represent SEM. $^*p < 0.05$, two-way ANOVA.

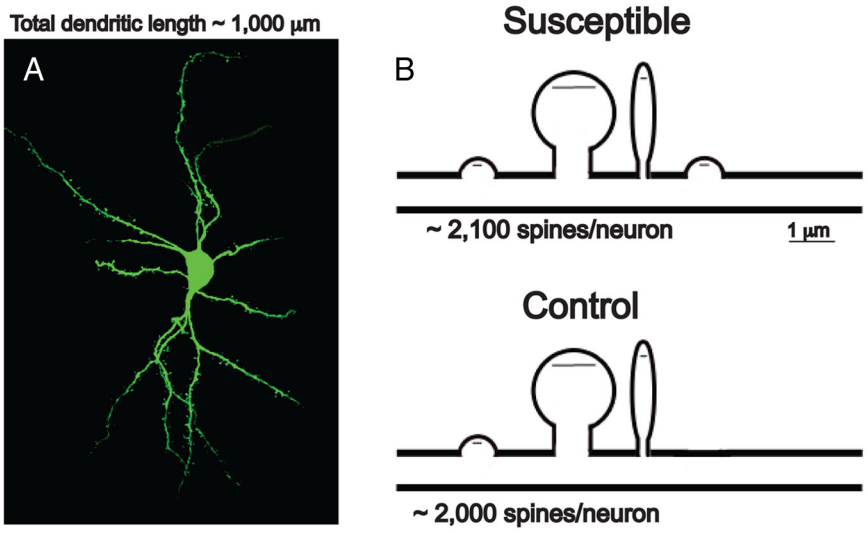

Figure 7. ***A***, Representative confocal image of an MSN. Average total dendritic length ($n = 5$ neurons) is 948.36 ± 115.19 μm. ***B***, Schematic representation of the effect of chronic social defeat stress on MSN spines. Small black lines in spine head represent the PSD. Social defeat results in approximately double the total number of stubby spines.

mice and demonstrate it to be an essential regulator of stress-induced structural and behavioral plasticity.

Changes in dendritic spine density and morphology are thought to underlie important aspects of experience-dependent plasticity (Holtmaat and Svoboda, 2009). Previous studies have shown that stress alters spine density in the hippocampus and amygdala (Vyas et al., 2004, 2006; Mitra et al., 2005), but we show here that stress regulates stubby spine structures in the NAc. Although less is known about these stubby structures, they have been shown to predominate early in postnatal development (Boyer et al., 1998) and to proliferate on mature hippocampal slices after blocking synaptic transmission (Petrak et al., 2005). In Parkinson's disease models, in which there is a depletion of dopaminergic input, there is a selective elimination of glutamatergic synapses (Day et al., 2006). It is possible that the increase in stubby spines may represent a homeostatic mechanism resulting from the increased firing and subsequent "shrinkage" of VTA dopaminergic neurons (Krishnan et al., 2007; Mazei et al., 2010). Approximately 70% of dopaminergic MSN synapses in the NAc shell occur on the dendritic shaft (Zahm, 1992). Therefore, activation of dendritic dopamine receptors, via increased VTA firing, could subsequently regulate the initiation of stubby spine formation. Interestingly, dopamine receptors are also located on the spine neck in the perisynaptic space (Smith and Bolam, 1990; Ferré et al., 2007). Therefore, stubby spines that lack a neck likely also have abnormal distributions of dopamine receptors in this space and might be more responsive to glutamatergic inputs, of which the NAc shell receives a substantial innervation from subcortical limbic structures (Zahm and Brog, 1992). Additionally, the spine neck is critical in isolating biochemical and electrical signals from the parent dendrite (Majewska et al., 2000; Araya et al., 2006). Stubby spines, with no neck, have stronger calcium signaling coupling with the parent dendrite and are involved in the regulation of spino-dendritic crosstalk (Schmidt and Eilers, 2009). The increase of ~130 stubby spines per neuron in susceptible mice likely has significant effects on MSN function and ultimately on social avoidance. This and many other hypotheses are currently being tested to determine the specific role of these new stubby glutamatergic synapses on neuronal signaling in the NAc.

In concert with these structural changes, we observed significant upregulation of total IKK protein, as well as an increase in total and phosphorylated IκB, its downstream target, indicating an increase in the signaling of this pathway. IKK acts to phosphorylate IκB, leading to its degradation and a release of inhibition on NFκB (Mercurio et al., 1999), which is known to play a role in synaptic plasticity and to regulate neuronal morphology (Meffert et al., 2003; Gutierrez et

al., 2005; Russo et al., 2009b). Previous studies have found that the IKK–NFκB signaling pathway is important for hippocampal neuroplasticity and in regulating memory consolidation (Meffert et al., 2003; Kaltschmidt et al., 2006; O'Mahony et al., 2006; Lubin and Sweatt, 2007). Additionally, we have shown that expression of IKKdn and IKKca can reduce and increase, respectively, total spine density of NAc MSNs (Russo et al., 2009b). Collectively, these data indicate that IKK is a key regulator of synaptic connectivity and brain function and likely plays a role in a number of psychiatric disorders.

A growing number of studies show similarities in plasticity mechanisms that promote susceptibility to addiction and stress-related disorders. Chronic cocaine and social defeat stress both increase spine density in the NAc (Robinson and Kolb, 1999; Nestler, 2001). Stress and cocaine also similarly increase strength of excitatory synapses on VTA dopamine neurons (Saal et al., 2003). Behaviorally, chronic cocaine and social defeat stress both sensitize animals to subsequent cocaine exposure, and, conversely, chronic cocaine increases susceptibility to social stress (Covington and Miczek, 2005; Covington et al., 2010). Furthermore, there also seems to be a commonality in some of the molecular mechanisms controlling behavioral and synaptic plasticity in addiction and stress disorders. Consistent with data shown here, expression of IKKdn in mouse NAc MSNs blocks cocaine-induced formation of spines and its rewarding effects (Russo et al., 2009a). Given that the NAc shell responds to both rewarding and aversive stimuli (Barrot et al., 2002), changes in the structure and function of NAc MSNs may strengthen the associated behaviors rather than directly driving them. The NAc shell is considered to be a limbic–motor interface that is responsible for integrating the salience of rewarding and aversive stimuli through its target brain regions (Mogenson et al., 1980; Meredith et al., 2008; Chen et al., 2010). For example, the strong innervations of the shell from the amygdala may partly explain its role in mediating stress-induced fear or aversion (Wright et al., 1996). In the case of drug abuse, dendritic spine changes may lead to exaggerated responses to the rewarding properties of the drug, whereas similar changes in dendritic structure after stress may lead to exaggerated responses to aversive stimuli associated with the stress. All of these results point to overlapping mechanisms responsible for stress- and drug-induced morphological plasticity, which strengthens our hypothesis that alterations in neuronal morphology control maladaptive behaviors in these psychiatric disorders.

Although it is clear from this work that structure and function of MSN synapses is altered by chronic stress, the specific molecular composition of these synapses is not known. Recent work has shown alterations in AMPA receptor subunit composition as a result of chronic stress (Campioni et al., 2009; Vialou et al., 2010). Additionally, studies of cocaine exposure and withdrawal have shown alterations in spine type and AMPA receptor composition over time (Ghasemzadeh et al., 2003; Boudreau and Wolf, 2005; Boudreau et al., 2007; Kourrich et al., 2007; Conrad et al., 2008; Pacchioni and Kalivas, 2009). These data indicate dynamic changes in spine size and synaptic AMPAR composition during the course of withdrawal. It will be important for future studies to determine the impact of chronic stress on the receptor composition and functional output of these newly formed stubby spine structures on NAc MSNs.

In summary, we provide strong evidence that chronic social defeat stress induces social avoidance by creating new spine structures on NAc MSNs, associated with increased mEPSC frequency, through an IKK-dependent mechanism. Futures studies to investigate the detailed time course and molecular composition of these new synapses will guide the development of therapeutics to target these adaptive plasticity mechanisms to control psychiatric dysfunction in depressive and related disorders.

References

Araya R, Jiang J, Eisenthal KB, Yuste R (2006) The spine neck filters membrane potentials. Proc Natl Acad Sci U S A 103:17961–17966.

Barrot M, Olivier JD, Perrotti LI, DiLeone RJ, Berton O, Eisch AJ, Impey S, Storm DR, Neve RL, Yin JC, Zachariou V, Nestler EJ (2002) CREB activity in the nucleus accumbens shell controls gating of behavioral responses to emotional stimuli. Proc Natl Acad Sci U S A 99:11435–11440.

Berton O, Nestler EJ (2006) New approaches to antidepressant drug discovery: beyond monoamines. Nat Rev Neurosci 7:137–151.

Berton O, McClung CA, Dileone RJ, Krishnan V, Renthal W, Russo SJ, Graham D, Tsankova NM, Bolanos CA, Rios M, Monteggia LM, Self DW, Nestler EJ (2006) Essential role of BDNF in the mesolimbic dopamine pathway in social defeat stress. Science 311:864–868.

Boudreau AC, Wolf ME (2005) Behavioral sensitization to cocaine is associated with increased AMPA receptor surface expression in the nucleus accumbens. J Neurosci 25:9144–9151.

Boudreau AC, Reimers JM, Milovanovic M, Wolf ME (2007) Cell surface AMPA receptors in the rat nucleus accumbens increase during cocaine withdrawal but internalize after cocaine challenge in association with altered activation of mitogen-activated protein kinases. J Neurosci 27:10621–10635.

Bourne J, Harris KM (2007) Do thin spines learn to be mushroom spines that remember? Curr Opin Neurobiol 17:381–386.

Boyer C, Schikorski T, Stevens CF (1998) Comparison of hippocampal dendritic spines in culture and in brain. J Neurosci 18:5294–5300.

Campioni MR, Xu M, McGehee DS (2009) Stress-induced changes in nucleus accumbens glutamate synaptic plasticity. J Neurophysiol 101:3192–3198.

Chakravarthy S, Saiepour MH, Bence M, Perry S, Hartman R, Couey JJ, Mansvelder HD, Levelt CN (2006) Postsynaptic TrkB signaling has distinct roles in spine maintenance in adult visual cortex and hippocampus. Proc Natl Acad Sci U S A 103:1071–1076.

Chen BT, Hopf FW, Bonci A (2010) Synaptic plasticity in the mesolimbic system: therapeutic implications for substance abuse. Ann N Y Acad Sci 1187:129–139.

Conrad KL, Tseng KY, Uejima JL, Reimers JM, Heng LJ, Shaham Y, Marinelli M, Wolf ME (2008) Formation of accumbens GluR2-lacking AMPA receptors mediates incubation of cocaine craving. Nature 454:118–121.

Covington HE 3rd, Miczek KA (2005) Intense cocaine self-administration after episodic social defeat stress, but not after aggressive behavior: dissociation from corticosterone activation. Psychopharmacology (Berl) 183:331–340.

Covington HE, Maze I, Bradbury K, Sun H, Mouzon E, Ghose S, Neve RL, Tamminga C, Nestler EJ (2010) A role for repressive histone methylation in cocaine-induced vulnerability to stress. Soc Neurosci Abstr 36:886.5.

Day M, Wang Z, Ding J, An X, Ingham CA, Shering AF, Wokosin D, Ilijic E, Sun Z, Sampson AR, Mugnaini E, Deutch AY, Sesack SR, Arbuthnott GW, Surmeier DJ (2006) Selective elimination of glutamatergic synapses on striatopallidal neurons in Parkinson disease models. Nat Neurosci 9:251–259.

Ferré S, Agnati LF, Ciruela F, Lluis C, Woods AS, Fuxe K, Franco R (2007) Neurotransmitter receptor heteromers and their integrative role in 'local modules': the striatal spine module. Brain Res Rev 55:55–67.

Geinisman Y, Gundersen HJ, van der Zee E, West MJ (1996) Unbiased stereological estimation of the total number of synapses in a brain region. J Neurocytol 25:805–819.

Ghasemzadeh MB, Permenter LK, Lake R, Worley PF, Kalivas PW (2003) Homer1 proteins and AMPA receptors modulate cocaine-induced behavioural plasticity. Eur J Neurosci 18:1645–1651.

Goldwater DS, Pavlides C, Hunter RG, Bloss EB, Hof PR, McEwen BS, Morrison JH (2009) Structural and functional alterations to rat medial prefrontal cortex following chronic restraint stress and recovery. Neuroscience 164:798–808.

Gutierrez H, Hale VA, Dolcet X, Davies A (2005) NF-kappaB signalling

regulates the growth of neural processes in the developing PNS and CNS. Development 132:1713–1726.
Harris KM, Kater SB (1994) Dendritic spines: cellular specializations imparting both stability and flexibility to synaptic function. Annu Rev Neurosci 17:341–371.
Holtmaat A, Svoboda K (2009) Experience-dependent structural synaptic plasticity in the mammalian brain. Nat Rev Neurosci 10:647–658.
Janssen WG, Vissavajjhala P, Andrews G, Moran T, Hof PR, Morrison JH (2005) Cellular and synaptic distribution of NR2A and NR2B in macaque monkey and rat hippocampus as visualized with subunit-specific monoclonal antibodies. Exp Neurol 191 [Suppl 1]:S28–S44.
Kaltschmidt B, Ndiaye D, Korte M, Pothion S, Arbibe L, Prüllage M, Pfeiffer J, Lindecke A, Staiger V, Israël A, Kaltschmidt C, Mémet S (2006) NF-kappaB regulates spatial memory formation and synaptic plasticity through protein kinase A/CREB signaling. Mol Cell Biol 26:2936–2946.
Kauer JA, Malenka RC (2007) Synaptic plasticity and addiction. Nat Rev Neurosci 8:844–858.
Kessler RC, Berglund P, Demler O, Jin R, Merikangas KR, Walters EE (2005) Lifetime prevalence and age-of-onset distributions of DSM-IV disorders in the National Comorbidity Survey Replication. Arch Gen Psychiatry 62:593–602.
Koo JW, Russo SJ, Ferguson D, Nestler EJ, Duman RS (2010) Nuclear factor-kappaB is a critical mediator of stress-impaired neurogenesis and depressive behavior. Proc Natl Acad Sci U S A 107:2669–2674.
Kourrich S, Rothwell PE, Klug JR, Thomas MJ (2007) Cocaine experience controls bidirectional synaptic plasticity in the nucleus accumbens. J Neurosci 27:7921–7928.
Krishnan V, Han MH, Graham DL, Berton O, Renthal W, Russo SJ, Laplant Q, Graham A, Lutter M, Lagace DC, Ghose S, Reister R, Tannous P, Green TA, Neve RL, Chakravarty S, Kumar A, Eisch AJ, Self DW, Lee FS, Tamminga CA, Cooper DC, Gershenfeld HK, Nestler EJ (2007) Molecular adaptations underlying susceptibility and resistance to social defeat in brain reward regions. Cell 131:391–404.
LaPlant Q, Chakravarty S, Vialou V, Mukherjee S, Koo JW, Kalahasti G, Bradbury KR, Taylor SV, Maze I, Kumar A, Graham A, Birnbaum SG, Krishnan V, Truong HT, Neve RL, Nestler EJ, Russo SJ (2009) Role of nuclear factor kappaB in ovarian hormone-mediated stress hypersensitivity in female mice. Biol Psychiatry 65:874–880.
Lubin FD, Sweatt JD (2007) The IkappaB kinase regulates chromatin structure during reconsolidation of conditioned fear memories. Neuron 55:942–957.
Majewska A, Brown E, Ross J, Yuste R (2000) Mechanisms of calcium decay kinetics in hippocampal spines: role of spine calcium pumps and calcium diffusion through the spine neck in biochemical compartmentalization. J Neurosci 20:1722–1734.
Mazei MS, Krishan V, Neve RL, Russo SJ, Nestler EJ (2010) Alteration in the morphology of dopaminergic neurons in the ventral tegmental area in response to social defeat stress. Soc Neurosci Abstr 36:886.12.
Meffert MK, Chang JM, Wiltgen BJ, Fanselow MS, Baltimore D (2003) NF-kappa B functions in synaptic signaling and behavior. Nat Neurosci 6:1072–1078.
Mercurio F, Murray BW, Shevchenko A, Bennett BL, Young DB, Li JW, Pascual G, Motiwala A, Zhu H, Mann M, Manning AM (1999) IkappaB kinase (IKK)-associated protein 1, a common component of the heterogeneous IKK complex. Mol Cell Biol 19:1526–1538.
Meredith GE, Baldo BA, Andrezjewski ME, Kelley AE (2008) The structural basis for mapping behavior onto the ventral striatum and its subdivisions. Brain Struct Funct 213:17–27.
Mitra R, Jadhav S, McEwen BS, Vyas A, Chattarji S (2005) Stress duration modulates the spatiotemporal patterns of spine formation in the basolateral amygdala. Proc Natl Acad Sci U S A 102:9371–9376.
Mogenson GJ, Jones DL, Yim CY (1980) From motivation to action: functional interface between the limbic system and the motor system. Prog Neurobiol 14:69–97.
Nestler EJ (2001) Molecular basis of long-term plasticity underlying addiction. Nat Rev Neurosci 2:119–128.
Nicholson DA, Geinisman Y (2009) Axospinous synaptic subtype-specific differences in structure, size, ionotropic receptor expression, and connectivity in apical dendritic regions of rat hippocampal CA1 pyramidal neurons. J Comp Neurol 512:399–418.
O'Mahony A, Raber J, Montano M, Foehr E, Han V, Lu SM, Kwon H, LeFevour A, Chakraborty-Sett S, Greene WC (2006) NF-kappaB/Rel regulates inhibitory and excitatory neuronal function and synaptic plasticity. Mol Cell Biol 26:7283–7298.
Pacchioni AM, Kalivas PW (2009) The role of AMPAR trafficking mediated by neuronal pentraxins in cocaine-induced neuroadaptations. Mol Cell Pharmacol 1:183–192.
Paxinos G, Franklin K (1997) The mouse brain in stereotaxic coordinates. San Diego: Academic.
Petrak LJ, Harris KM, Kirov SA (2005) Synaptogenesis on mature hippocampal dendrites occurs via filopodia and immature spines during blocked synaptic transmission. J Comp Neurol 484:183–190.
Radley JJ, Rocher AB, Miller M, Janssen WG, Liston C, Hof PR, McEwen BS, Morrison JH (2006) Repeated stress induces dendritic spine loss in the rat medial prefrontal cortex. Cereb Cortex 16:313–320.
Robinson TE, Kolb B (1999) Alterations in the morphology of dendrites and dendritic spines in the nucleus accumbens and prefrontal cortex following repeated treatment with amphetamine or cocaine. Eur J Neurosci 11:1598–1604.
Rodriguez A, Ehlenberger DB, Dickstein DL, Hof PR, Wearne SL (2008) Automated three-dimensional detection and shape classification of dendritic spines from fluorescence microscopy images. PLoS One 3:e1997.
Russo SJ, Mazei-Robison MS, Ables JL, Nestler EJ (2009a) Neurotrophic factors and structural plasticity in addiction. Neuropharmacology 56 [Suppl 1]:73–82.
Russo SJ, Wilkinson MB, Mazei-Robison MS, Dietz DM, Maze I, Krishnan V, Renthal W, Graham A, Birnbaum SG, Green TA, Robison B, Lesselyong A, Perrotti LI, Bolaños CA, Kumar A, Clark MS, Neumaier JF, Neve RL, Bhakar AL, Barker PA, Nestler EJ (2009b) Nuclear factor κB signaling regulates neuronal morphology and cocaine reward. J Neurosci 29:3529–3537.
Russo SJ, Dietz DM, Dumitriu D, Morrison JH, Malenka RC, Nestler EJ (2010) The addicted synapse: mechanisms of synaptic and structural plasticity in nucleus accumbens. Trends Neurosci 33:267–276.
Saal D, Dong Y, Bonci A, Malenka RC (2003) Drugs of abuse and stress trigger a common synaptic adaptation in dopamine neurons. Neuron 37:577–582.
Schmidt H, Eilers J (2009) Spine neck geometry determines spino-dendritic cross-talk in the presence of mobile endogenous calcium binding proteins. J Comput Neurosci 27:229–243.
Shansky RM, Morrison JH (2009) Stress-induced dendritic remodeling in the medial prefrontal cortex: effects of circuit, hormones and rest. Brain Res 1293:108–113.
Shepherd GM, Pologruto TA, Svoboda K (2003) Circuit analysis of experience-dependent plasticity in the developing rat barrel cortex. Neuron 38:277–289.
Smith AD, Bolam JP (1990) The neural network of the basal ganglia as revealed by the study of synaptic connections of identified neurones. Trends Neurosci 13:259–265.
Thomas MJ, Beurrier C, Bonci A, Malenka RC (2001) Long-term depression in the nucleus accumbens: a neural correlate of behavioral sensitization to cocaine. Nat Neurosci 4:1217–1223.
Tsankova NM, Berton O, Renthal W, Kumar A, Neve RL, Nestler EJ (2006) Sustained hippocampal chromatin regulation in a mouse model of depression and antidepressant action. Nat Neurosci 9:519–525.
Vialou V, Robison AJ, Laplant QC, Covington HE 3rd, Dietz DM, Ohnishi YN, Mouzon E, Rush AJ 3rd, Watts EL, Wallace DL, Iñiguez SD, Ohnishi YH, Steiner MA, Warren BL, Krishnan V, Bolaños CA, Neve RL, Ghose S, Berton O, Tamminga CA, Nestler EJ (2010) DeltaFosB in brain reward circuits mediates resilience to stress and antidepressant responses. Nat Neurosci 13:745–752.
Vyas A, Pillai AG, Chattarji S (2004) Recovery after chronic stress fails to reverse amygdaloid neuronal hypertrophy and enhanced anxiety-like behavior. Neuroscience 128:667–673.
Vyas A, Jadhav S, Chattarji S (2006) Prolonged behavioral stress enhances synaptic connectivity in the basolateral amygdala. Neuroscience 143:387–393.
Wright CI, Beijer AV, Groenewegen HJ (1996) Basal amygdaloid complex afferents to the rat nucleus accumbens are compartmentally organized. J Neurosci 16:1877–1893.
Zahm DS (1992) An electron microscopic morphometric comparison of tyrosine hydroxylase immunoreactive innervation in the neostriatum and the nucleus accumbens core and shell. Brain Res 575:341–346.
Zahm DS, Brog JS (1992) On the significance of subterritories in the "accumbens" part of the rat ventral striatum. Neuroscience 50:751–767.